Lanckriet, S., Tesfaalem Gebreyohannes, Frankl, A., Amanuel Zenebe, Nyssen, J., 2016. Sediment in alluvial and lacustrine debris fans as an indicator for land degradation around Lake Ashenge (Ethiopia). Land Degradation and Development, 27: 258 – 269.

ABSTRACT

Sediments deposited by (paleo) flash floods can hold valuable information on processes of environmental change, land degradation or desertification. In order to assess the suitability of flash flood deposits as proxies for land degradation, we monitored a representative gully segment in North Ethiopia (Ashenge catchment), investigated a sequence of alluvial debris fans downstream of this segment and dated a neighboring subaquatic debris fan using short-lived ^{210}Pb isotope counting. During one rainy season (July-September 2014), we measured daily rainfall, peak discharge, bedload transport, suspended sediment load and sediment deposition rates. The data show that sediment deposition in the debris fans is significantly dependent on micro-topography (net incision in micro-channels) ($p < 0.1$) and position within the sequence (net incision farther away from the lake) ($p < 0.05$). As sediment transfer to the lake significantly depends on the balance between available water and sediment (ratio rainfall depth / bedload transport) ($p < 0.05$), we could reconstruct the hydro-sedimentary evolution of the gully over the past half century and validate it with aerial photographs and semi-structured interviews. The findings are consistent with the short-lived isotope count results, indicating increased sediment supply from the 1970s onwards, when little amounts of clay were deposited in the lake (< 5%), and a subrecent clear water effect that resulted in increased deposition rates of clay in the lacustrine debris fan. Overall, our analysis indicates that debris fan sediments can be used to estimate past environmental degradation rates, if the contemporary water and sediment behavior is well understood.

Keywords: sediment – gully – hydrogeomorphology – ^{210}Pb – short-lived isotopes

1. INTRODUCTION

Sediment transport can be used as a valuable research 'proxy' for the assessment of environmental degradation in regions with a strongly contrasted climate (alternating wet and dry seasons). For instance, Vanmaercke et al. (2011) employ sediment yield as an effective desertification risk indicator. Avni (2005) also shows that gully sediment dynamics under

headcut retreat are a key factor for desertification in the Negev. In particular, it is recognized that sediment deposited in alluvial fans located downstream of ephemeral streams (Figure 1) can hold valuable information concerning environmental change and environmental degradation. Harvey (2012) claims that alluvial debris fans have not only a 'functional role' of control on sediment supply from hillslope gullies to stream channels, but have also a 'preservational role' as storage zones that contain information on (past) environmental change. Consequently, alluvial fan sediments could be equally useful as research 'proxies' for land degradation assessment, if their evolution responds to degradation in their catchments. Geomorphological studies on alluvial fans show that they are often built up (i) by sheetflood deposits (Sweeney and Loope, 2001), (ii) by sediment-charged flash floods (Blair, 1999, 2000), or (iii) by accumulation on the fan from supercritical standing waves of expanding sheetfloods (Blair, 2000).

FIGURE 1

Generally, the study of the driving forces of gullying is less developed in comparison with the study of their control technology and physical modelling (Carnicelli et al., 2009). Moreover, geomorphological studies often focus on soil erosion at hillslope scale and on conservation by means of trapping (see Mekonnen et al., 2014), while there is fewer information about such dynamics at gully or watershed scale (Grimaldi et al., 2013). Hence, debate concerning the driving forces of the morphologic evolution of alluvial debris fans is ongoing. Late Holocene anthropogenic impact leading to alluvial debris fan development is a common theme. For example, Chiverrell et al. (2007) attribute the late Holocene increase in gullying activity in Lancashire (Great Britain) to population expansion, a growing rural economy, and an increased anthropogenic pressure on upland hill slopes that are crucial in priming hill slopes before major storm events. Also, Eriksson et al. (2000) found that the recent phase of floodout aggradation (< 1000 years) in central Tanzania is probably the result of the introduction or intensification of agriculture and livestock husbandry. Other studies focus on climate change as the cause of alluvial fan evolution. For example, Lafortune et al. (2006) found that alluvial fans in Canada have been deposited by torrential activity, due to increasing rainfall or triggers that lower the precipitation threshold. Also Grenfell et al. (2012) found floodouts in the semi-arid Karoo region (South Africa) formed under increased precipitation. Others, such as Zygmunt (2009) attribute the development of alluvial fans to a combination of climatic changes and human impact. Additionally, some authors discuss the impact of gully's

'authigenic' factors, such as local conditions independent of external drivers, i.e. control of the hydraulic base level (Prosser et al., 1994; Bull, 1997; Carnicelli et al., 2009).

In North Ethiopia, the controlling factors of sediment dynamics in ephemeral streams are not yet fully understood. The flashfloods in these ephemeral streams have severe negative impacts on both the regional agricultural economy and human health. Overland flow and concentrated water flow can induce downstream flooding, high sediment concentration of the water and severe fluvial erosion. Unfortunately, measuring and modeling sediment transport in ephemeral streams is a rather difficult task, mainly due to the unpredictable nature of the flashfloods (Reid et al., 1996; 1998). Hydrological models are often equipped for predictions in perennial streams in the more temperate (humid) regions of the world, so they are often less accurate in areas with contrasted climatic conditions (Reid et al., 1995). Mechanisms of stream hydrology differ significantly between regions with different climates. For instance, Laronne & Reid (1993) show coarse bedload sediment transport in ephemeral streams can be up to 400 times more efficient than in humid perennial rivers.

For North Ethiopia in particular, several regional studies exist on the dynamics of soil loss (Yeshaneh et al., 2015; Mekonnen et al., 2015), soil nutrients (Mekuria and Aynekulu, 2013), runoff (Opolot et al., 2014), catchment sediment yield (Haregeweyn et al., 2013) or suspended sediment transport (Amanuel Zenebe, 2009; Vanmaercke et al., 2010), but to date few studies have been performed focusing on bedload transport. Further, it is not clear to what extent alluvial debris fans could be useful 'tools' to assess land degradation. Therefore, in this paper we will present (i) a characterization of water and sediment dynamics at a gully system near Lake Ashenge (North Ethiopia); (ii) empirical relations to express water and sediment dynamics in terms of their controlling factors; (iii) short-lived isotope dating of a subaquatic debris fan; and (iv) a reconstruction of land degradation processes from a sequence of alluvial debris fans found downstream of the gully system.

2. METHODS

2.1 Study catchment of Ashenge

Our study was performed within a gully catchment adjacent to Lake Ashenge (North-Ethiopia), close to the city of Korem (12°30'N, 39°31'E) within the region of Tigray (Figure 2). Lake Ashenge is situated in a marginal graben bounded by NNE-SSW faults, formed

parallel to and higher up than the larger Raya graben. Geology consists of Tertiary volcanics, in particular the trap basalts of the Ashangi group, which are black alkali olivine basalts (Paleocene, Oligocene and Miocene) with frequent intercalations of silicified limestone in-between (Merla et al., 1979). Quaternary basin fill (gravels to clays) is composed of eluvial, colluvial and alluvial material, as well as of paleo lacustrine sediments to the North of the current lake and near Korem (Kurkura Kabeto et al., 2012). Later, a number of gullies incised the valley bottom around the graben lake and several of them bear debris fans downstream at the lake shore (Frankl et al., 2011). Upper catchments have overall high slopes gradients (0.5 to 1.0 m m^{-1}) while near to the lake gentle gradients occur (< 0.1 m m^{-1}). Average yearly rainfall is ~900 mm yr^{-1} (station of Maychew) (Frankl et al., 2011) but precipitation is concentrated in the months between June and September when very high rainfall intensities occur. Most catchments have forested upper parts but are in general dominated by croplands, while grazing occurs on grasslands close to the lake. Land tenure was long organized according to feudal principles, but was restructured after the civil war (1974-1991) (Lanckriet et al., 2014a).

The first studied 'Menkere gully' (site 1) lies adjacent to the village of Menkere, to the East of the lake (Figure 2). Upstream, the gully incises rather shallow colluvium on steep slopes. Downstream, the gully incises a flat but thick alluvial-colluvial mantle. The gully catchment is mainly composed of croplands, with some areas of woody vegetation on the steeper slopes. In the gully, a sequence of three debris fans is evident (coded DF1 to DF3) and one additional fan extends into the lake (DF4, at the closest position by the lake) (Figure 1 & 2). Just Northeast of DF4, a conical spot of grazing lands most probably also corresponds to an inactive debris fan (Figure 2), although this could not be clearly substantiated on the field. Cross-sections of the debris fans show that they are built-up by stony debris (Figure 1b). The gully catchment has an area of 221 ha. The second studied 'Korem gully' (site 2), with a catchment of 193 ha, lies south of the lake, where a large underwater debris fan is present (Figure 2).

2.2 Measurement campaign

Following Gould (1987), an in-depth assessment of contemporary hydro sedimentary processes now in operation is a prerequisite for understanding past sedimentary behavior. Upstream of the depositional area, the Menkere gully was instrumented (Figure 2) in order to understand the contemporary sediment dynamics during flashfloods in the rainy season (July-

September 2014). Measurements included (i) rainfall, (ii) peak discharge, (iii) bed load transport, (iv) suspended sediment load and (v) spatially distributed sediment deposition rates.

FIGURE 2

2.2.1 Rainfall measurements

Rainfall was measured by a rain gauge installed about 100 m from the gully channel (Figure 2) and monitored twice a day (at 8 AM and 6 PM). The standard rain gauge, made of a metal cylindrical funnel, was installed level and in an open field, far away from any obstacles (Figure 3a).

2.2.2 Peak discharge measurements

Due to the instantaneous nature of the floods, excessive velocities and accessibility problems, direct measurement of flash floods in ephemeral rivers is usually impractical when they occur. Peak discharges can, however, be indirectly estimated after floods using crest stage gauges (Tesfaalem et al., 2015). Peak flow height was therefore monitored for floods during July, August and September 2014 (Figure 3b). Peak discharge was recorded by a crest stage gauge with floating marker (sawdust) installed at a rectangular gully segment near the village (segment width 8.1 m) (S in Figure 2). We follow the recommendations made by Tesfaalem et al. (2015) by installing the gauge level in a straight, permanent and stable channel section. Small floods with flow heights less than 20 cm could not be measured, but the 20 cm was added when calculating peak depths. We computed peak discharges (Q_p; m^3/s) from peak depths using the Manning equation, with R the hydraulic radius (m), A the flow area (m^2), S the channel slope (0.02) and a roughness coefficient n estimated at 0.030 (Chow, 1959):

$$Q_p = \frac{AR^{2/3}\sqrt{S}}{n} \quad (1)$$

2.2.3 Measurement and characterization of daily bedload transport

After every flood, the volume of transported bed load material was measured in a cemented sediment trap placed in the active gully channel (Figure 2). The construction (dimensions of 2.4 m by 0.4 and 0.5 m) consisted of three small traps (dimensions of 0.4 m by 0.4 m and 0.5 m) that occupied 37 % of the channel bottom width; this was done in order to minimize interference of the installation with the measurement of downstream bed load sediment deposition rates (Figure 3c). Measured sediment volumes (n = 30) were multiplied by a

conversion parameter ζ calculated as the ratio of the length of the construction with the combined length of the traps. The construction was placed just downstream of the staff gauge, with the longest side perpendicular on the channel direction. We took three random samples of the bedload sediment using Kopecky rings (5.1 cm height, 5 cm across, 100 cm^3 volume), in order to estimate sediment bulk density. We estimate the bedload sediment trapping efficiency of the traps at ~ 100 %, i.e. the fraction of the sediment that enters the trap and which is deposited in the trap (Verstraeten & Poesen, 2001). This is because the traps were never fully filled during one event and the combined trap volume of 0.24 m^3 > the measured volume of trapped sediments (always < 0.20 m^3, with only once an exception of 0.23 m^3). This sediment also included pebbles, so we counted the number of trapped pebbles (NTP) in the construction after every flood and following the Wentworth US Geological Survey grain size chart characterized them as cobbles (diameter > 6.4 cm), very coarse pebbles (diameter 3.2 – 6.4 cm) and coarse pebbles (diameter 3.2 – 1.6 cm).

2.2.4 Characterization of suspended sediment load

During two floods, three samples of suspended sediment load were taken in the flood at intervals of five minutes during the peak flood. For this purpose, two-liter bottles were installed on a long metal stake and a depth-integrated sample was taken in the middle of the water flow (Figure 2; Figure 3d). In order to allow water to move into the bottles at a controlled rate, the opening of the bottles was turned away from the direction of the water flow. All samples were filtered in a funnel with Whatman 42 filter paper (pore size of 2.5 µm), oven-dried and sediment was weighed in order to determine suspended sediment loads (Mekele University Soil Laboratory).

2.2.5 Vertical sediment deposition rates and magnitude of downstream transfer

Vertical sediment deposition rates were determined by vertical measurements relative to 45 stable markers installed in the four depositional areas (DF1-DF4) (Figure 2; Figure 3e). Measurement was performed twice a week and hence debris fan volume changes could be calculated (mean vertical change multiplied with debris fan area; m^3). For every marker, the position in the gully bed was noted (in a micro channel or on a micro ridge), as well as the number of the debris fan in which it was located (coded DF1 to DF4). Analysis of variance allowed calculation of sediment deposition rates in terms of these factors. We also ranked all

events on a scale of ‘magnitude of downstream transfer’ (MDT), with value 5 if overall deposition occurs in the lake (i.e. overall incision of all debris fans taken together) and values 1 to 4 if deposition is starting from DF1 to DF4 respectively onwards. Moreover, we coded all events according to their ‘sediment transfer to the lake’ (STL) (1 if the total debris fan volume change was negative, which represents net erosion of the debris fans with sedimentation in the lake; 0 if the change was positive).

FIGURE 3

2.3 Alluvial debris fan sequence

As stated before, a sequence of four alluvial fans was found downstream of the staff gauge. It is possible that these debris fans may deliver information on past land degradation upstream, if the contemporary sediment dynamics of the gully system are well understood. We followed the methodology of Lanckriet et al. (2014a), based on the AGERTIM method developed by Nyssen et al. (2006), in order to assess the temporal evolution of the fan complex, semi-structured interviews in and around the gully sites were performed with 14 farmers. The farmers were interviewed independently and individually, during walks along the gully. The interviewees were asked to show and locate the features they were talking about. These included the occurrence and timing of appearance of, among others, boulders, alluvial fans, floods, gully incisions and terraces. Only if all interviewed farmers came independently and individually to the same conclusions were these insights used in the study.

In order to independently assess the chronology of the debris fan sequence development, aerial photographs of the area were obtained. These include aerial photographs taken in 1936, 1965, 1986 and recent images. Each set of the 1936 photographs contains one vertical photograph, two low-oblique photographs and one high-oblique photograph, taken simultaneously at a flight height of about 4000-4500 m a.s.l., resulting in a scale of about 1:16 000 - 1:18 000 (low-oblique photographs) (Nyssen et al., 2015). We used a low-oblique photograph of the study area and lakeshore (Table 1) which could be compared to the aerial photographs of 1965, 1986 and to high resolution CNES/Astrium images accessible on Google® Earth.

TABLE 1

2.4 Subaquatic debris fan

Additional dating of debris fan dynamics around Lake Ashenge was derived from short-lived isotope counting. For logistical reasons, no subaquatic alluvial fan sample could be taken near the Menkere gully. Therefore, we focused on the second gully downstream of a gully system located at the South of the lake (Korem gully), where an underwater debris fan is present (Figure 2). Using a gravity corer (Uwitec, 2014) from a boat, a subaquatic debris fan sample was collected approximately 100 m from the shore and in alignment with the gully channel, over a depth of 16 cm. This core of shallow lake sediments was retrieved and sectioned upright with a fixed-interval sectioning device in 1-cm slices.

Using a high-purity Germanium detector (Centre d'Etudes Nordiques; Québec, Canada), supported isotopes of ^{210}Pb and non-supported ^{210}Pb were measured for samples taken at 2 cm intervals. Sediment age was estimated using the constant-rate-of-supply model, assuming a constant atmospheric lead flux under varying sediment supply (Appleby, 1978).

Sediment texture was determined for all 16 subsamples. Treatment with 35% hydrogen peroxide allowed removal of the organic matter, whereafter sand (>63 µm) was separated from silt and clay (<63 µm) by wet sieving of the sample with distilled water on a 63 µm sieve. The sandy fraction was measured, and some 2.5-3 g of the remaining silt and clay fraction was mixed with a 40 ml 0.2% sodium hexametaphosphate solution, and treated with ultrasound. Texture of the clayey and silty classes was then determined in the UGent sedimentology laboratory with X-ray sedigraphy (*SediGraph III Plus*), a methodology based on the combined laws of Beer-Lambert and Stokes. Reynolds numbers were held between 0.3 and 0.5 to ensure laminarity of the suspension (Micromeritics, 2014).

3. RESULTS

3.1 Characterization of the hydro-sedimentary regime

3.1.1 Rainfall distribution and peak discharges

Rainfall in 2014 was rather ‘late’, since the first real storms arrived only at the end of July (Figure 4). Apart from the delayed start, measured storms were quite typical for the region, with maximum daily rainfall amounts up to 40 mm. These values are generally in line with the data described by Nyssen et al. (2005), who measured for instance a maximum rain depth over 1 h (32 mm) that is only slightly less than that over 24 h (34 mm). Note that most rainfall

was recorded as nighttime rain (*in casu* 3.4 times as much as compared to daytime rain) and that precipitation was highest in August (Figure 4a). There were also 10 dry days in the middle of the rainy season; a t-test showed that the average daily rainfall before (8.2 mm) and after (8.4 mm) this period was not significantly different ($p > 0.1$). Using the Manning method we calculated peak discharges that range between 4.65 and 19.00 m^3/s, with an average of 7.93 ± 5.46 m^3/s. There are only few peak discharge data ($n = 7$), partly due to theft of the gauge in the middle of the rainy season (one week of missing data). We could model peak discharges from the following significant relationship between peak discharge (Q_p) and R_{24} (cumulative rainfall over the past 24 hours):

$$Q_p = 0.3592 R_{24} \qquad (n = 7;\ p < 0.05;\ R^2 = 0.25) \qquad (2)$$

3.1.2 Suspended sediment and bedload transport

Suspended sediment load was measured for six samples during two floods and was on average 18.3 ± 10.9 g/l, which is broadly in the range of the suspended sediment load data reported for ten catchments in the Highlands by Vanmaercke et al. (2010). Taking the average peak discharge into account (7.93 m^3/s), we estimate the average suspended sediment load at peak flood around 145.1 kg/s.

Sampled bedload was mostly sand and amounted to 3.1 m^3 over the entire rainy season; on average 0.10 ± 0.06 m^3 per flood. Taking into account the conversion parameter ζ of 2.67 and the average bulk density of 1.59 g/cm^3, this represents 13.2 tonnes over the rainy season or an average of 425 kg of bedload transport per flood (Figure 4). In total, 72 trapped pebbles were counted, of which most (43 %) were characterized as 'coarse pebbles', and the rest as 'cobbles' (31 %) and 'very coarse pebbles' (26 %). The pebbles account only for a very small portion of the total bedload volume and most pebbles were counted in August, except for a period of ten days with absence of any sediment and pebble activation during the already mentioned dry spell (4-13 August 2014) (Figure 4). Two t-tests showed that neither bed load sediment nor the number of trapped pebbles per day differed significantly ($p > 0.1$) before and after this dry spell.

FIGURE 4

3.1.3 Sediment deposition rates in debris fans

Vertical depth measurements relative to the markers allowed identification of both erosion and deposition patterns within the debris fans. In general, the gully segment is in a rather stable geomorphic equilibrium, given that for all markers there was an average vertical evolution of - 0.17 cm per flood. Generally, most deposition occurred during the first big floods (the end of July), while important phases of erosion were common over the whole rainy season. As indicated by the mean vertical changes (cm) and debris fan volume changes (m^3) per event, depositional variability appears to be higher in the upper debris fans while eroded and deposited volumes are larger for DF4 (Figure 5).

FIGURE 5

3.2 Impact of discharge on sediment transport

There is a well-studied and strong relation between discharge Q and suspended sediment load (SSC) in the North Ethiopian Highlands (Amanuel Zenebe, 2009; Vanmaercke et al., 2010). We also find a very strong relation between peak discharge (Q_p) and the number of trapped pebbles NTP (Pearson product-moment correlation = 0.97). The following equation could be established:

$$NTP = 0.3751 Q_p + 0.0731 \qquad (R^2 = 0.94;\ p < 0.05) \qquad (3)$$

The relationships between Q_p and the number of trapped pebbles taking into account pebble sizes, as well as between Q_p and bed load transport (BT) (m^3) were weaker and not significant. Moreover, there is no tendency in bed load transport volumes apparent over the rainy season (Figure 4). However, a significant logarithmic relation was identified between antecedent 24h-rainfall (R_{24}) and bedload transport. Hence, even under relatively small amounts of rainfall (R_{24} < 10 mm), bed load transport (BT, in m^3) can be substantial:

$$BT = 0.0289 \log(R_{24}) + 0.0279 \qquad (R^2 = 0.19,\ p < 0.05) \qquad (4)$$

3.3 Factors controlling sediment deposition

3.3.1 Sediment deposition as controlled by microtopography

Mean deposition per flood in micro channels was compared with mean deposition per flood on micro ridges, by means of a non-parametric t-test. Mean vertical change in micro-channels over the rainy season was - 0.49 cm per marker per flood (net incision), while it was + 0.07 cm per marker per flood (net aggradation) on the micro-ridges. The difference between both means is significant at the 0.1 level (p = 0.09).

3.3.2 Sediment deposition as controlled by fan location

Analysis of variance showed that mean deposition on at least one debris fan was significantly different from mean deposition on other debris fans (p < 0.05). Post-hoc analysis with non-parametric t-tests allowed further characterization. Mean deposition on DF4 was + 0.038 cm per marker per flood, while this was - 0.077 cm on DF3, - 0.005 cm on DF2 and - 0.059 cm on DF1. Only the difference between DF4 (overall net deposition) and the other debris fans (overall net incision) is significant (p = 0.03). Interestingly, the current deposition is in DF4 while the sediment is channeled through DF1, DF2 and DF3 that are eroded out. An upstream

clear water effect can hence facilitate sediment deposition further downstream, a situation that was also observed on larger scale in the nearby Gra Kashu catchment (Tesfaalem et al., 2015).

3.3.3 Downstream sediment transfer as controlled by the water-sediment balance

A t-test shows that the ratio rainfall depth / bedload transport is significantly higher during events with 'sediment transfer to the lake' (ratio = 55.7), as compared to events where the sediment is essentially deposited in the debris fans (ratio = 8.4) ($p < 0.05$). The 'magnitude of downstream transfer' is strongly and positively correlated with the ratio rainfall depth / bed load transport (Spearman rank-order correlation = + 0.78). Assuming equal intervals (presuming that the distances between ordinal scores are equal; Howell, 1997), linear regression facilitated explanation of the 'magnitude of downstream transfer' by the ratio rainfall depth / bedload transport ($p < 0.05$; $R^2 = 0.50$). Thus, significantly more sediment is transferred downstream or towards the lake if rainfall (modeled peak discharge) is high; or if the amount of mobilized bedload in the channels is relatively low ('clearer water').

3.4 Short-lived isotope counts

Changes in gully activity over 70 years could be derived from the short-lived isotope counting of the subaquatic lacustrine debris fan (Table 2). Overall, ^{210}Pb isotope values are low, probably resulting from the semi-arid climatic conditions. The unsupported ^{210}Pb, transported from the gully watershed, increases from the bottom of the core towards 7 cm, then stays roughly constant up to the top of the core. Assuming a constant-rate-of-supply, dates were calculated (Table 2). Mass-median-diameter (D_{50}), silty fractions and clay fractions give an indication of sediment flux activity (Figure 6). At 7-9 cm depth, there are higher abundances of coarser silty grains, while almost no clay is deposited at that time (~ 1980s). The deposition rates increase gradually over time and accelerate after the 1980s (Figure 6).

TABLE 2

FIGURE 6

3.5 Farmers' assessments on the age of debris fan deposition

No farmers remembered the earliest period (before 1950) and few farmers remembered the period before the 1970s or their answers were considered to be inconsistent. During the 1970s to the 1990s, the biggest debris fan adjacent to the lake (DF4) appeared. According to all

farmers, DF4 is considered as the oldest deposit (~ 30-40 years). Several farmers state that a deep gully was then located at the place of DF1, DF2 and DF3. Later, around the year 2000, the second biggest debris fan (DF3) appeared, just upstream of DF4. The appearance of DF2 was estimated around 2005-2010, as was DF1.

To date, the debris fans remain active. The farmers point at a continuing growth of DF3 and DF4, among others by stating that 'DF3 was much smaller ten years ago, as it was partly a grazing land'; and that 'DF4 is becoming wider and wider over recent years'.

3.6 Changes to gully and debris deposition, as retrieved from aerial photographs

Lake Ashenge is visible on the earliest aerial photograph (1936). Around the lake, no debris fans can be seen while the photo also shows a house surrounded by trees just to the southwest of the studied gully. These are still visible on the 1965 photograph, while a shallow sediment accumulation (located at the current position of DF3) developed just downstream of a small channel incision near the house and along a line of euphorbias (Figure 7). These elements are no longer visible on the aerial photograph of 1986, depicting a debris fan further downstream at the lake shore. While there is no sign of other shallow zones or debris fans along the gully, a broader incision is present at the location of the former sediment accumulation (DF3) that was visible on the 1965 photograph (Figure 7). Some farmlands that were visible near the lake on the 1965 photograph were covered with sediment in 1986. The CNES-Astrium images show the current situation, while DF3 reappears on the image, two other debris fans appear more upstream and DF4 covers a larger area than in 1986 (Figure 7).

FIGURE 7

3.7 Chronology of alluvial debris fan evolution

Linking the semi-structured interviews, the sequence of aerial photographs, the ^{210}Pb isotope dating and the significantly positive relation between magnitude of downstream transfer and discharge/sediment, facilitates the reconstruction of the sedimentary evolution of the gully since the 1930s (Table 3). Conceptually, we identify five different sedimentary "periods"; in so doing, we show that flashflood sediments can be useful proxies for land degradation.

TABLE 3

3.7.1 Sedimentary Phase I (1930s – 1950s): low peak discharges

As there are no debris fans visible on the early aerial photograph, and given the relatively high proportions of clay in the shallow core (Figure 6), the first half of the 20th century was a period with relatively low peak discharges. According to Frankl et al. (2011), upslope gullies around Ashenge were stabilized during this period. Land use in the upper catchment was already dominated by cereal agriculture, but many trees and shrubs were present on lynchets, steep slopes and in the stream bed.

3.7.2 Sedimentary Phase II (1960s – 1970s): increasing discharges and sediment supply

The mass-median-diameter of the shallow core peaks at 50 µm during the 1970s (Figure 6). The aerial photograph shows sediment accumulation along the gully at the current location of DF3 (Figure 7), although there is no sign of debris fans at the lake shore. This must have been a period with predominantly higher discharges and sediment supply from the catchment. Upslope gullies were still quite stable, with a position of the lower gully end similar to the 1930s (Frankl et al., 2011). These authors infer a drainage density of 22.26 m ha^{-1} in a nearby catchment around Lake Ashenge in 1965.

3.7.3 Sedimentary Phase III (1970s – 1990s): high discharges

The interview records on this period are in line with the appearance of DF4 on the aerial photograph of 1986, while the former sediment accumulation (DF3) gets incised. This indicates a period with predominantly high discharges and high amounts of sediment towards DF4 and the lake. During the 1980s, the subaquatic debris cone contains more coarse grains, shown by higher proportions of silty grains (up to 85 %) (Figure 6). At the same time, only a small proportion of clay was present in the core (< 10 %). These findings are in line with the observations of Frankl et al. (2011), who identify incision in the lower valley floor with a sediment fan in a neighboring catchment by 1975. Eleven years later, the lowest gully end was located more downstream with a drainage density of 24.96 m ha^{-1}. A debris fan is then clearly visible (Frankl et al., 2011).

3.7.4 Sedimentary Phase IV (2000s): upslope migrating debris cones

Following the interviews and the appearance of DF1 and DF2, the debris fans are developing as an "upslope migrating" sequence, during a period with decreasing discharges. While DF4 continues to grow and DF3 reappears, the upper sections of the shallow lake core contain

again higher relative amounts of clay (Figure 6). By 2009, the drainage density of the neighboring catchment was 24.59 m ha^{-1} (Frankl et al., 2011).

3.7.5 Sedimentary Phase V (2010's): observations of a clear water effect

We observed recent gully incision activity, indicative of even lower amounts of sediment supply towards the gully segment. In particular, DF1 and DF2 are incised by a channel, according to all farmers no older than 3 years. About 100 m upstream of DF1, this young channel incises the former gully bottom, resulting in a small terrace sculpted in the alluvio-colluvial mother mantle. Under decreased amounts of upstream sediment supply, a clear water effect can explain the increased deposition rates under decreased mass-median-diameters at the subaquatic Korem gully debris fan during this period (Figure 6), probably originating from activation of finer micro-channel material.

4. DISCUSSION

4.1 Co-evolution of erosional and depositional phases

The evolution of alluvial fan sedimentation corresponds well with periods of gully erosion and drainage density of gully channels identified by Frankl et al. (2011, 2013). These authors could detect three broad periods of gully erosion over the 20th century, by studying historical terrestrial and aerial photographs: (i) a stage with stable first order channels 1886-1965; (ii) a stage with activation of first order streams 1965-2000; and (iii) a stage of de-activation of first order streams 2000-present (Frankl et al., 2011, 2013). Their first stage of first order channel stability correlates well with Phase I of our sediment supply history; as is their second stage similar with our Phases II and III; and their third stage with our Phases IV and V. Such findings are also broadly in line with longer-term gully dynamics over the past millennia, as Lanckriet et al. (2014a) relate phases of downstream valley aggradation in the Northeastern Highlands with increases in sediment supply and upstream erosive activity. Taking the co-evolution of erosional and depositional phases together, we conceive an 'accordion' system – illustrating the connectivity between both upstream and downstream channel ends. During periods with stable upstream channels, downstream no sedimentation occurs. During periods with active upstream channels and retreating gully heads, or when a clear water effect is present (eroding out the upstream debris fans), progressive downstream sedimentation occurs.

Under an ‘intermediate’ regime, the system of debris fans can migrate downstream or upstream. This kind of geomorphic behavior is in line with general alluvial fan theory (Knighton, 1998; Graf, 2002). Broadly, alluvial fans develop when channel widening allows for channel migration (e.g. at the Ashenge shore) and when upland erosion increases the sediment supply (Graf, 2002). Indeed, the upland basin is the main sediment source for fan growth, notably when sediment production is high compared to sediment transport capacity (Knighton, 1998). These results are also in line with the theory of Exner (1920, 1925) that the rate erosion/deposition in a stream segment is proportional to the gradient of water flow velocity in the segment (Exner, 1925) and negatively related with the rate of bed load transport from upstream (Exner, 1920).

4.2 Relation with land policies, drought and the Ashenge lake level

The phases of alluvial fan accumulation as identified in this study and the phases of active gully erosion as identified by Frankl et al. (2011, 2013) also correlate well with changes in North Ethiopian land policies. Lanckriet et al. (2014a) describe three main political-ecology eras (the late feudal era, the civil war and the post-revolution era), each with a specific configuration of land and conservation policies. Under the late feudal land system the *mwufar* sharecropping system discouraged investments in land conservation and poor farmers had to farm on steeper slopes. In the nearby Gra Kashu catchment, the proportion of cropland was at its maximum and occupied very steep slopes during the 1960s, when there was a minimum of woody vegetation (De Meyere et al., 2015). Indeed, based on historical land use and land cover mapping with warped terrestrial photographs from around Menkere, Meire (2009) shows that bushland cover was higher in 1936 (29.6% of the total land cover) as compared to 1961 (26.8%), while cropland cover was lower in 1936 (64.8%) as compared to 1961 (73.2%). Between 1961 and 2008, cropland cover declined again to the level of 1936, while bushland cover declined further to 25.4%. Overall, cropland cover around Menkere was at its maximum during the 1960s (late feudal era) (Meire, 2009). The pre-1980 appearance of sediment fans and the peaking mass-median-diameters in the subaquatic debris then result from the degraded socio-environmental situation inherited from that late-imperial period (Sedimentary Phase II).

Further, appearance of alluvial fans (Sedimentary Phase III) during the eighties coincided with the civil war, economic decline and a lack of investment in conservation efforts (Lanckriet et al. 2014a). After a period of relatively high rainfall, a series of droughts struck the decade of

the 1980s, as influenced by the interplay of several oceanic oscillations (Lanckriet et al., 2014b). This must have had an impact on the Ashenge Lake level; Schuett and Busschert (2005) report high lake levels during the 1930s and 1960s, 10 m above present levels, based on oral evidence. The lake level was low during the 1980s with lake levels about 5 m lower than present (Ethiopian Ministry of Water and Energy; data courtesy of Enyew Adgo, Bahir Dar University). Hence, the hydraulic base level lowered, further facilitating gully incision. Today the lake has risen as indicated by drowned trees near the western shore (Schuett and Busschert, 2005). After the regime change in 1991, intensive conservation efforts (Lanckriet et al., 2014a) clearly succeeded in a reduction and overall stabilization of sediment supply (Sedimentary Phases IV and V).

5. CONCLUSIONS

In this integrated study of hydro sedimentary changes around Lake Ashenge, we identified distinct sedimentary periods over the past decades: (i) a period of sedimentary stability in the early 20th century; (ii) a period of sedimentary destabilization in the 1960s – 1970s; (iii) a phase of sedimentary instability in the 1970s – 1980s; (iv) a phase of upslope migrating debris cones in the 1990s – 2000s; and finally (v) a period with more clear water effects (2010s). During phases of retreating gully heads, progressive downstream sedimentation occurs in the alluvial debris fans, while 'clearer water' results in increased deposition of finer sediment particles in the lake. The periods of active gully sedimentation correlate well with periods of intensive gully erosion and clearly co-evolve with periods of decreased vegetation cover under insecure land tenure, drought and lower base levels. These findings corroborate the usefulness of sediments in alluvial and lacustrine debris fans as adequate proxies for paleo environmental and land degradation analyses.

Acknowledgements:

This study became possible thanks to the support of our translator Bereket and of Anthony Denaeyer, the support of our data collectors Hayelom and Meles, the help of Etefa Guyassa and the funding by UGent's Special Research Fund. Special thanks go to Dr. Sébastien Bertrand for his help on the lead dating, to the fishermen of Lake Ashenge for providing boat transport, to the Mekele University Soil Laboratory for the suspended sediment load analysis, to the UGent sedimentology laboratory and to the dating laboratory of the Centre d'Etudes Nordiques (Québec, Canada).

6. REFERENCES

Amanuel Zenebe. 2009. Assessment of spatial and temporal variability of river discharge sediment yield and sediment-fixed nutrient export in Geba River catchment northern Ethiopia. Unpublished PhD thesis KULeuven.

Appleby P. 1978. The calculation of lead-210 dates assuming a constant rate of supply of unsupported 210Pb to the sediment. *Catena* **5** (1): 1–8.

Avni Y. 2005. Gully incision as a key factor in desertification in an arid environment the Negev highlands Israel. *Catena* **63** (2-3): 185-220.

Blair T. 1999. Sedimentology of the debris-flow-dominated Warm Spring Canyon alluvial fan Death Valley California. *Sedimentology* **46**: 941-965.

Blair T. 2000. Sedimentology and progressive tectonic unconformities of the sheetflood-dominated Hell's Gate alluvial fan Death Valley California. *Sedimentary Geology* **132**: 233-262.

Bull W. 1997. Discontinuous ephemeral streams. *Geomorphology* **19**: 227–276.

Carnicelli S, Benvenuti M, Ferrari G, Sagri M. 2009. Dynamics and driving factors of late Holocene gullying in the Main Ethiopian Rift (MER). *Geomorphology* **103** (4): 541-554.

Chiverrell R, Harvey A, Foster G. 2007. Hillslope gullying in the Solway Firth – Morecambe Bay region Great Britain: Responses to human impact and/or climatic deterioration? *Geomorphology* **84**: 317-343.

Chow V. 1959. Open-channel hydraulics: New York McGraw-Hill 680 p.

De Meyere M, Tesfaalem Asfaha, Nyssen J. 2015. Runoff variability as impacted by physiographical factors and spatio-temporal changes in land use and cover: A case on the Rift Valley escarpment of Northern Ethiopia. *Soil Use and Management*: in preparation.

Eriksson M, Olley J, Payton R. 2000. Soil erosion history in central Tanzania based on OSL dating of colluvial and alluvial hillslope deposits. *Geomorphology* **36**: 107-128.

Exner F. 1920. Zur physik der dunen. *Akad. Wiss. Wien Math. Naturwiss*. **129**: 929-952.

Exner F. 1925. Uber die Wechselwirkung zwischen Wasser und Geschiebe in Flussen. *Akad. Wiss. Wien Math. Naturwiss.* **134**: 165-203.

Frankl A, Nyssen J, De Dapper M, Haile M, Billi P, Munro N, Deckers J, Poesen J. 2011. Linking long-term gully and river channel dynamics to environmental change using repeat photography (Northern Ethiopia). *Geomorphology* **129**: 238-251.

Frankl A, Poesen J, Mitiku Haile, Deckers J, Nyssen J. 2013. Quantifying long-term changes in gully networks and volumes in dryland environments: the case of Northern Ethiopia *Geomorphology* **201**: 254–263.

Gould S. 1987. Time's Arrow, Time's Cycle: Myth and Metaphor in the Discovery of Geological Time. Harvard University Press, USA: 119p.

Graf W. 2002. Fluvial processes in dryland rivers. The Blackburn Press Caldwell USA.

Grenfell S, Rowntree K, Grenfell M. 2012. Morphodynamics of a gully and floodout system in the Sneeuberg Mountains of the semi-arid Karoo South Africa: Implications for local landscape connectivity. *Catena* **89**: 8-21.

Grimaldi S, Angeluccetti I, Coviello V, Vezza P. 2013. Cost-Effectiveness Of Soil And Water Conservation Measures On The Catchment Sediment Budget - The Laaba Watershed Case Study, Burkina Faso. *Land Degradation & Development*: in press. DOI: http://dx.doi.org/10.1002/ldr.2212.

Haregeweyn N, Poesen J, Verstraeten G, Govers G, de Vente J, Nyssen J, Deckers J, Moeyersons J. 2013. Assessing the performance of a Spatially distributed soil erosion and sediment delivery model (WATEM/SEDEM) in Northern Ethiopia. *Land Degradation and Development* **24**: 188-204.

Harvey A. 2012. The coupling status of alluvial fans and debris cones: a review and synthesis. *Earth Surface Processes and Landforms* **37**: 64-76.

Howell D. 1997. Statistical methods in psychology (4th ed.). Duxbury Press Belmont USA.

Knighton D. 1998. Fluvial forms and processes a new perspective. Hodder Education London UK.

Kurkura Kabeto, Aynalem Zenebe, Bheemalingeswara K, Kinfe Atshbeha, Solomon Gebresilassie, Kassa Amare. 2012. Mineralogical and Geochemical Characterization of Clay and Lacustrine Deposits of Lake Ashenge Basin Northern Ethiopia: Implication for Industrial Applications. *Momona Ethiopian Journal of Science (MEJS)* **4** (2): 111-129.

Lafortune V, Filion L, Hétu B. 2006. Impacts of Holocene climatic variations on alluvial fan activity below snowpatches in subarctic Québec. *Geomorphology* **76**: 375-391.

Lanckriet S, Derudder B, Naudts J, Bauer H, Deckers J, Mitiku Haile, Nyssen J. 2014a. A political ecology perspective of land degradation in the North Ethiopian Highlands. *Land Degradation and Development*. DOI: 10.1002/ldr.2278

Lanckriet S, Frankl A, Enyew Adgo, Termonia P, Nyssen J. 2014b. Droughts related to quasi-global oscillations: a diagnostic teleconnection analysis in North Ethiopia. *Int. J. Climatology*. DOI: 10.1002/joc.4074.

Laronne J, Reid I. 1993. Very high bedload sediment transport in desert ephemeral rivers. *Nature* **366**: 148-150.

Meire E. 2009. Mapping of land use and cover in the North Ethiopian highlands since 1868 using warped terrestrial photographs. Unpublished MSc Dissertation, Ghent University, Department of Geography.

Mekonnen M, Keesstra S, Stroosnijder L, Baartman J, Maroulis J. 2014. Soil conservation through sediment trapping: A review. *Land Degradation & Development*: in press. DOI: 10.1002/ldr.2308.

Mekonnen M, Keesstra S, Baartman J, Ritsema C, Melesse A. 2015. Evaluating sediment storage dams: structural off-site sediment trapping measures in northwest Ethiopia. *Cuadernos de Investigación Geográfica* **41** (1): 7-22.

Mekuria W, Aynekulu E. 2013. Exclosure land management for restoration of the soils in degraded communal grazing lands in Northern Ethiopia. *Land Degradation and Development* **24** (6): 528-538.

Merla G, Abbate E, Azzaroli A, Bruni P, Canuti P, Fazzuoli M, Sagri M, Tacconi P. 1979. A Geological Map of Ethiopia and Somalia (1973). 1:2000.000; and Comment. University of Florence Firenze.

Micromeritics. 2014. http://www.micromeritics.com/ (accessed on 14/05/2014)

Nyssen J, Vandenreyken H, Poesen J, Moeyersons J, Deckers J, Haile Mitiku, Salles C, Govers G. 2005. Rainfall erosivity and variability in the Northern Ethiopian Highlands. *J. Hydrology* **311**: 172–187.

Nyssen J, Poesen J, Veyret-Picot M, Moeyersons J, Mitiku Haile, Deckers J, Dewit J, Naudts J, Kassa Teka, Govers G. 2006. Assessment of gully erosion rates through interviews and measurements: a case study from northern Ethiopia. *Earth Surface Processes and Landforms* **31** (2): 167–185.

Nyssen J, Petrie G, Sultan Mohamed, Gezahegne Gebremeskel, Frankl A, Stal C, Seghers V, Debever M, Demaeyer Ph, Kiros Meles Hadgu, Billi P, Mitiku Haile. 2015. Historical aerial photographs of Ethiopia in the 1930s and their fusion with current remotely sensed imagery for retrospective geographical analysis. *Journal of Cultural Heritage:* submitted.

Opolot E, Araya T, Nyssen J, Al-Barri B, Verbist K, Cornelis, W. 2014. Evaluating in situ water and soil conservation practices with a fully coupled, surface/subsurface process-based hydrological model in Tigray, Ethiopia. *Land Degradation & Development*. DOI: 10.1002/ldr.2335.

Prosser I, Chappell J, Gillespie R. 1994. Holocene valley aggradation and gully erosion in headwater catchments southeastern highlands of Australia. *Earth Surface Processes and Landforms* **19**: 465–480.

Reid I, Laronne J. 1995. Bedload sediment transport in an ephemeral stream and comparison with seasonal and perennial counterparts. *Water Resources Research* **31**: 773-781.

Reid I, Powell D, Laronne J. 1996. Prediction of bedload transport by desert flash-floods. *Journal of Hydraulic Engineering of the American Society of Civil Engineers* **122**: 170-173.

Reid I, Laronne J, Powell D. 1998. Flash-flood and bedload dynamics of desert gravel-bed streams. *Hydrological processes* **12**: 543-557.

Schuett B, Busschert R. 2005. Geomorphological reconstruction of palaeo Lake Ashengi Northern Ethiopia. Lake Abaya Research Symposium Proceedings: 51-57.

Sweeney M, Loope D. 2001. Holocene dune-sourced alluvial fans in the Nebraska Sand Hills. *Geomorphology* **38**: 31-46.

Tesfaalem G, Asfaha Frankl A, Mitiku Haile, Nyssen J. 2015. Catchment rehabilitation and hydro-geomorphic characteristics of mountain streams in the western Rift Valley escarpment of Northern Ethiopia. *Land Degradation and Development*. DOI: 10.1002/ldr.2267.

Uwitec. 2014. http://www.uwitec.at/ (accessed on 9/12/2014)

Vanmaercke M, Amanuel Zenebe, Poesen J, Nyssen J, Verstraeten G, Deckers J. 2010. Sediment dynamics and the role of flash floods in sediment export from medium-sized catchments: a case study from the semi-arid tropical highlands in northern Ethiopia. *Journal of Soils and Sediments* **10** (4): 611-627.

Vanmaercke M, Poesen J, Verstraeten G, Maetens W, de Vente J. 2011. Sediment yield as a desertification risk indicator. *Science of the Total Environment* **409**: 1715-1725.

Verstraeten G, Poesen J. 2001. Modelling the long-term sediment trap efficiency of small ponds. *Hydrological Processes* **15**: 2797–2819.

Yeshaneh E, Salinas J, Blöschl G. 2015. Decadal trends of soil loss and runoff in the Koga Catchment, Northwestern Ethiopia. *Land Degradation and Development*. DOI: 10.1002/ldr.2375.

Zygmunt E. 2009. Alluvial fans as an effect of long-term man-landscape interactions and moist climatic conditions: A case study from the Glubczyce Plateau SW Poland. *Geomorphology* **108**: 58-70.

FIGURES

Figure 1: Alluvial debris fans along the Menkere gully, including (a) the fan adjacent to the lake (coded DF4 in Figure 2) (the lake is at the back of the photographer and euphorbia trees are approximately 3 m high); and (b) a profile on the stoniness of DF2. See the sheep for indication of scale.

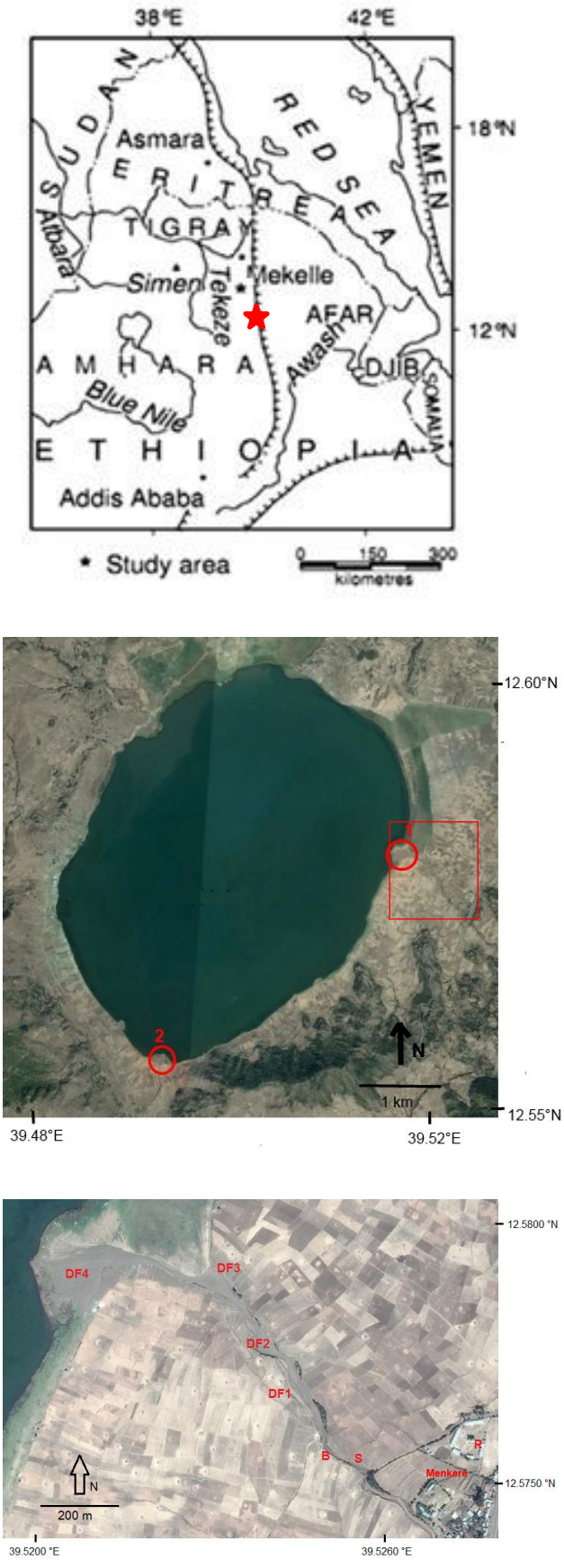

Figure 2. Location of the study area (indicated with red star) and the two study sites (1 indicates the Menkere gully and 2 indicates the Korem gully) (upper photo); and location of

the debris fans (DF4, DF3, DF2, DF1) at study site 1 (lower image), where sediment deposition rates were monitored, as well as the location of the bed load trap (B), the staff gage and suspended sediment sampling (S) and the rain gage (R). Background is given by CNES-Astrium images (18/01/2014) and the village of Menkere is indicated. The area covered by Figure 7 is indicated by a red rectangle.

Figure 3. Monitoring installations for sediment dynamics, including (a) the rain gage, (b) the crest stage gage, (c) bedload trap, (d) sampler for suspended sediment load measurements, and (e) a stable vertical marker as indicated with blue paint. The sediment deposition was measured relative to the lowest line of blue paint.

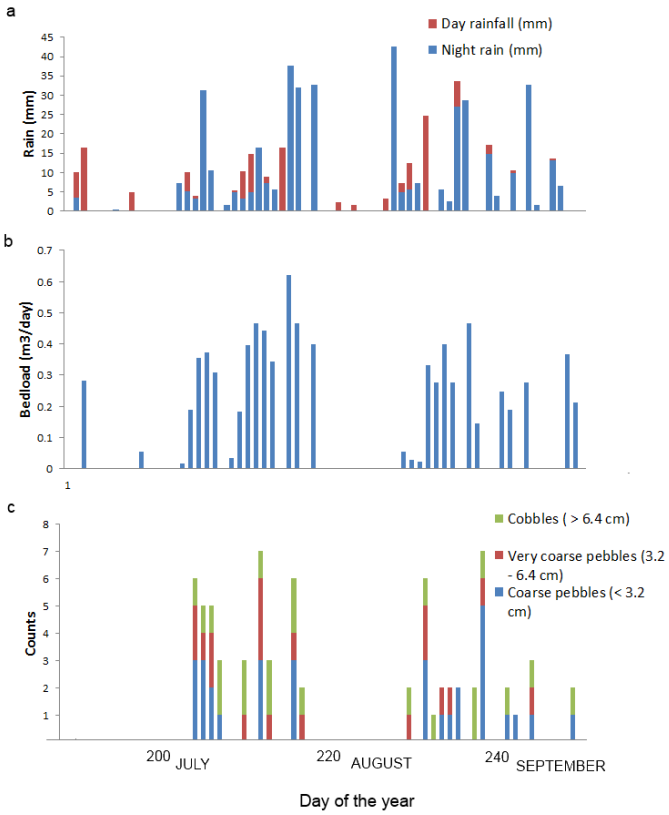

Figure 4. Temporal patterns (in 2014) of (a) daily rainfall (in mm/day); (b) computed bed load transport (m^3/day); (c) number of trapped pebbles per day.

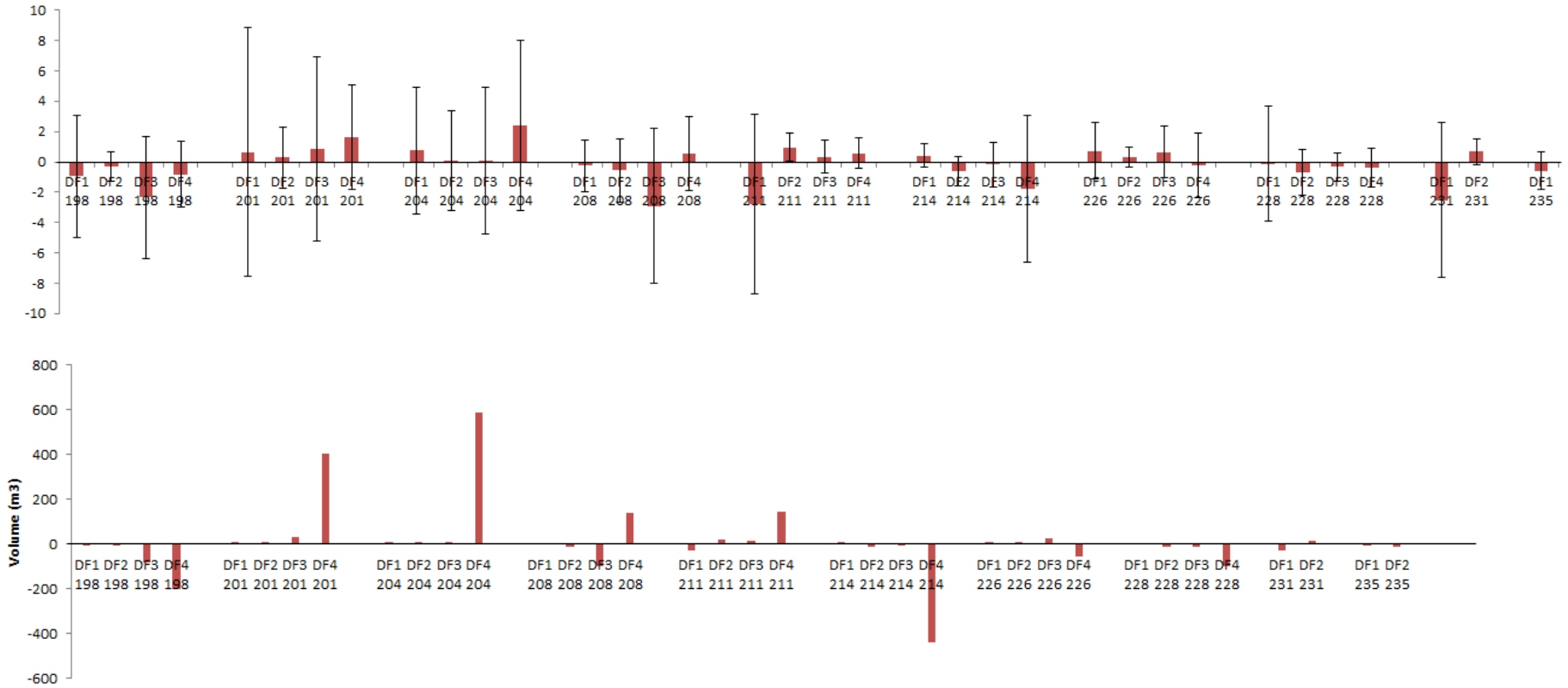

Figure 5. Mean vertical changes (cm) and volume changes (m^3) on all debris fans, in days of the year with indication of standard deviation. Days 231 and 235 show some missing data.

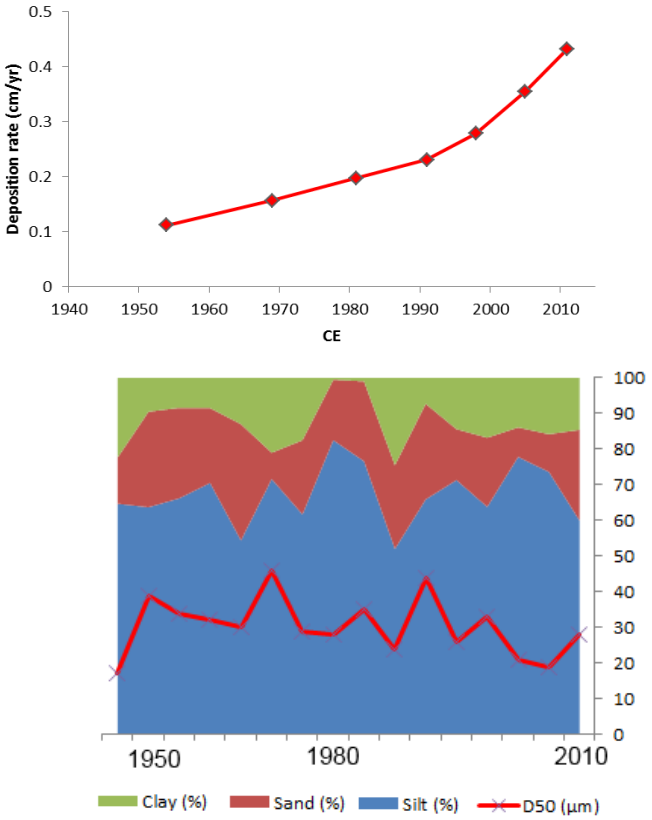

Figure 6. (left) Deposition rates (cm/yr) in function of time of deposition (middle of the time interval between two dates) show the recent effect of 'clearer water'; (right) D_{50} (µm), sandy, silty and clayey fraction (in %) in function of time show decreasing clay deposition around the 1980s.

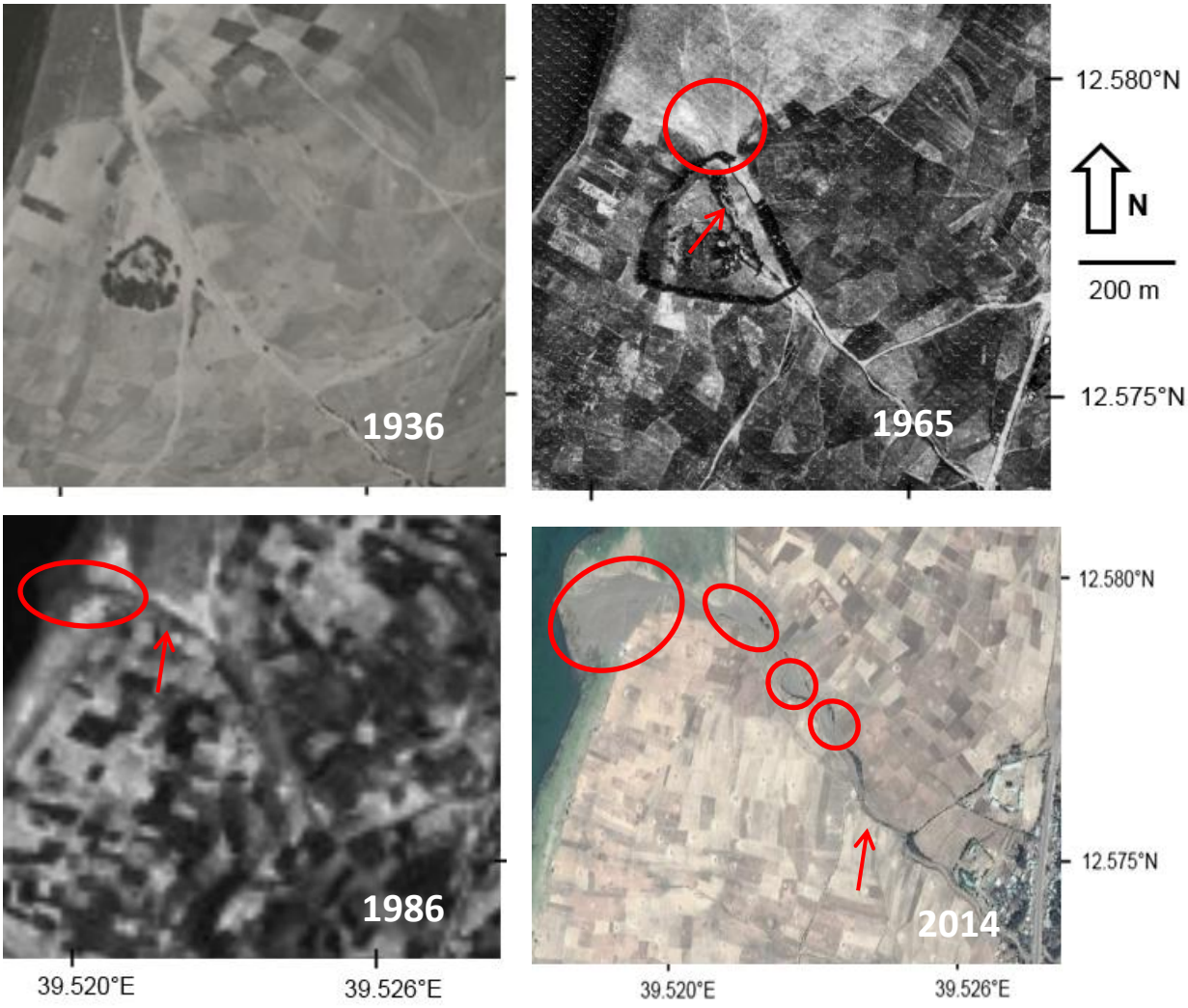

Figure 7. The Menkere gully as visible on the aerial photographs of 1936 (up left), 1965 (up right), 1986 (down left) and 2014 (down right). Minor flat zones (sediment accumulations) are indicated with red circles; active incisions with red arrows.

TABLES

Table 1. Remote sensing images (aerial photographs and satellite images) used to study the alluvial fan sequence development.

Image	Date	Operator	Source	Resolution
109-103 (flight of 24-03-1936)	March 1936	Istituto Geografico Militare	Geography Department, Ghent University	ground resolution < 2 m
24OCT65-R-187-186 96	October 1965	Swedsurvey	Ethiopian Mapping Agency	ground resolution of ca. 1.9 m
13NOV86-S12-01-0043	November 1986	Swedsurvey	Ethiopian Mapping Agency	ground resolution of ca. 1.9 m
CNES/Astrium images	January 2014	GeoBasis – DE/BKG	Google® Earth	ground resolution of ca. 0.5 m

Table 2. ^{210}Pb dating results (based on the constant-rate-of-supply model) of the subaquatic lacustrine debris fan; as well as mass-median-diameter of the sediment (D50, in µm).

Depth (cm)	^{210}Pb activity (Bq/g)	^{226}Ra daughters (Bq/g)	^{210}Pb unsupported (Bq/g)	Error ^{210}Pb unsupported (mBq/g)	*Pb age with error (CE)*	D_{50} (µm)
1	0.103245	0.008189	0.096452	12	2013	28.2
2						19.0
3	0.108447	0.005513	0.104454	11	2010 ± 2.1	21.4
4						33.3
5	0.115254	0.009735	0.107086	12	2005 ± 2.3	26.1
6						44.1
7	0.104155	0.004496	0.101165	12	1998 ± 2.5	24.7
8						35.3
9	0.082415	0.010037	0.073478	11	1989 ± 2.7	28.1
10						29.6
11	0.073760	0.008922	0.065830	10	1979 ± 3.0	46.5
12						29.9
13	0.067482	0.006705	0.061718	9	1966 ± 3.5	32.0
14	0.088819	0.005531	0.084597	11	1948 ± 4.5	34.3
15						39.2

Table 3. Evidence for gully debris fan evolution since the 1930s.

Phase	Date	Available data	Sources
I	1930s-1950s	no debris fans apparent	aerial photograph 1936
		subaquatic clay deposition	short core
II	1960s-1970s	higher D_{50} in subaquatic core	short core
		sediment accumulation	aerial photograph 1965
III	1970s-1990s	appearance of DF4	aerial photograph 1986 / interviews
		subaquatic silt deposition	short core
IV	2000s	upslope migrating debris fans	interviews
		subaquatic clay deposition	short core
V	2010s	gully cut activity	field observations